2020 IEEE International Conference on Robotics and Automation (ICRA)
31 May - 31 August, 2020. Paris, France

Stability Criteria of Balanced and Steppable Unbalanced States for Full-Body Systems with Implications in Robotic and Human Gait

William Z. Peng, *Student Member, IEEE*, Carlotta Mummolo, *Member, IEEE*, and Joo H. Kim, *Member, IEEE*

***Abstract*— Biped walking involves a series of transitions between single support (SS) and double support (DS) contact configurations that can include both balanced and unbalanced states. The new concept of steppability is introduced to partition the set of unbalanced states into steppable states and falling (unsteppable) states based on the ability of a biped system to respond to forward velocity perturbations by stepping. In this work, a complete system-specific analysis of the stepping process including full-order nonlinear system dynamics is presented for the DARwIn-OP humanoid robot and a human subject in the sagittal plane with respect to both balance stability and steppability. The balance stability and steppability of each system are analyzed by numerical construction of its balance stability boundaries (BSB) for the initial SS and final DS contact configuration and the steppable unbalanced state boundary (SUB). These results are presented with center of mass (COM) trajectories obtained from walking experiments to benchmark robot controller performance and analyze the variation of balance stability and steppability with COM and swing foot position along the progression of a step cycle. For each system, DS BSBs were obtained with both constrained and unconstrained arms in order to demonstrate the ability of this approach to incorporate the effects of angular momentum and system-specific characteristics such as actuation torque, velocity, and angle limits.**

I. Introduction

Biped systems such as humanoid robots and humans are able to perform a wide variety of dynamic tasks and locomotion with enhanced versatility and agility relative to other types of mobile systems such as wheeled vehicles. However, biped systems are also subject to the ever present risk of falling and instability during walking and standing, which poses a major challenge in robotics research. The analysis of balance stability in biped systems presents a fundamental but difficult problem due to the dimensionality, redundancies, and complex environmental interactions inherent in these systems (Fig. 1).

The multiple approaches that have emerged to address this challenge fall into three major categories: ground reference point criteria, limit cycle stability, and capturability-based criteria. Common ground reference point criteria for the dynamic balance of a biped system include the zero-moment point (ZMP) and its extensions

*This work was supported in part by the U.S. National Science Foundation (CMMI-1436636 and IIS-1427193).

W. Z. Peng and J. H. Kim are with the Department of Mechanical and Aerospace Engineering at New York University, Brooklyn, NY, USA. (Corresponding author e-mail: joo.h.kim@nyu.edu)

C. Mummolo is with the Department of Biomedical Engineering at the New Jersey Institute of Technology, Newark, NJ, USA.

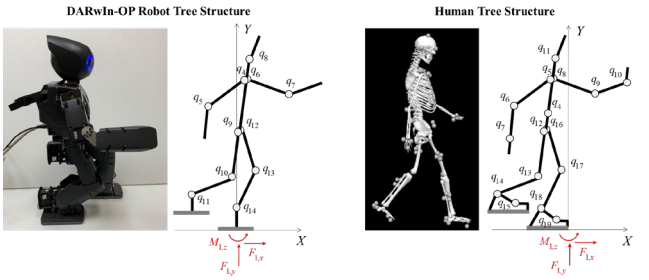

Figure 1. DARwIn-OP humanoid robot and human tree structure models in the sagittal plane

such as the foot rotation indicator (FRI) [1] [2]. These criteria are neither necessary nor sufficient conditions for balance [3] [4] because they do not consider the system's actuation torque, velocity, and variable limits; response to large perturbations; complete contact constraints; and other relevant physical components. Moreover, ground reference point criteria cannot easily be applied in general to other tasks and systems.

Limit cycle stability approaches to balance stability derived from nonlinear dynamical systems theory include Poincare maps [5], Lyapunov exponents [6], and sensitivity norms [7]. However, these are usually restricted to considering only local stability (i.e., the sensitivity of the biped system in response to infinitesimal perturbations [6]) with respect to a periodic gait or other specific motion. In general, the balance stability of a biped system subject to non-infinitesimal perturbations must be considered not only for periodic tasks such as walking and running, but also for general manipulation tasks such as lifting or throwing and aperiodic or non-steady gait.

Capturability-based analysis, which is based on the concept of a system's viability, has been introduced as a form of state-space-based criteria for balance stability through the mechanism of stepping. The viability kernel of a system is the set of all initial states from which there exists at least one evolution that never results in a failed or non-viable (unbalanced) state [8]. By definition, the state of a biped system is viable (balanced) if and only if it lies within the viability kernel of the system. However, the evaluation of the viability kernel is a computationally intractable problem for typical biped systems of interest due to the common issues of high dimensionality, nonlinearity, and the redundancy in the system dynamics and constraints [8] [9]. The evaluation of capturability, defined as the ability of a system to avoid ever reaching a failed state within a specified number of steps, presents a more tractable alternative. The set of capturable states can be computed to obtain a viable-capture basin for analysis rather than the full

viability kernel. Specifically, the *N*-step viable capture basin may be computed by only including *N*-step capturable states, states from which the biped system is able to come to a stop after taking at most *N* steps [9] [10].

Capturability-based approaches to balance stability typically resolve the issue of high dimensionality by considering either solely centroidal dynamics or relying on simplified reduced-order models of the original system. Along this direction, analytic treatments of capturability have been derived for reduced-order models such as the linear inverted pendulum model (LIPM) [11], where the necessary conditions on initial center of mass (COM) state (COM position and velocity) are known in the case of point feet and planar motion [12]. In the case of the LIPM with non-point feet, there exists a point where a contact force can be applied on the system in order to bring it to a statically stable configuration, defined as the capture point [13]. The capture point has been applied to the case of the 3-D LIPM in analyzing three-dimensional balance stability during walking, where it is referred to as the divergent component of motion [14]. Viable capture-basins have also been obtained for centroidal momentum planar walking models with sums-of-squares optimization in order to consider the angular momentum effect of swing limbs and upper body motion [15].

Although the scope of capturability-based approaches has expanded to explicitly consider swing leg dynamics [16], walking with variable COM height [17], and multi-contact situations [18], no capturability-based approach can fully incorporate all relevant information about a biped system while still remaining computationally tractable. Missing details include system-specific characteristics such as nonlinear actuation torque, velocity, and variable limits and aspects of the full-order, nonlinear system dynamics such as the complete angular momentum effect of swing limbs and upper body motion. The latter is difficult to fully model because the angular momentum generation capability of a swing limb also depends on system-specific characteristics such as the actuation torque, velocity, and variable limits. These additional details affect balance stability and successful swing foot placement, both of which are required for stepping during gait.

The objective of this work is to create a framework for analyzing a full step cycle in detail by combining analysis of the balance stability of the initial and final contact configurations, and the feasibility of contact transitions between the two configurations. The proposed approach can accurately demonstrate the effect of full-order, nonlinear system dynamics and the system-specific contributions (subject to model imperfections and uncertainties) of nonlinear actuation characteristics on balance stability in stepping. In addition, the approach applies to general systems and tasks.

II. Theoretical Framework

The conditions for balance used in capturability [19] inspired previous work toward a refined COM-state-space-based definition of balance with respect to a specific contact configuration. A system state is considered to be balanced if and only if it can indefinitely remain within its specified contact configuration (e.g., single support (SS) or double support (DS)) without necessarily modifying its contacts [20]. Otherwise, the necessity of modifying its current contacts is what defines an unbalanced state of the system. The balance stability boundary (BSB) is a partition of COM-state space (the space of COM position and velocity) into sets of balanced and unbalanced states with respect to a contact configuration. The BSB is found as the set of extremized COM states, which are the maximum allowable velocity perturbations at varying COM positions from which a biped system can still maintain its specified contact configuration [20]. The BSB framework of identifying COM-state-space partitions has been shown to be computationally tractable for both reduced- [21] [22] and full-order biped models that consider system-specific actuation torque, velocity, and variable limits [23] [20].

The concept of steppability is defined here as the ability of a biped system to achieve a desired step (i.e., SS to DS transition). Starting with the BSB, which partitions a biped system's entire COM-state space into balanced and unbalanced states, applying steppability as a condition further partitions the space of unbalanced states into steppable and falling (unsteppable) states depending on the feasibility of successful swing foot placement.

In that sense, steppability is a complementary concept to the existing concept of capturability. For example, given an initial COM state, the capture region for a biped indicates where a swing foot should be placed on the ground to recover from a given perturbation, which may be physically unrealizable due to restrictive joint kinematic limits or swing leg dynamics. Steppability addresses the opposite question: given that a particular step length has been achieved, steppability considers the set of all possible initial states from which the system could have originated.

For steppability, a partition of COM-state space is insufficient because the same COM state can be realized with different swing foot positions. Hence, the state space of the system considered for steppability is the COM-state space augmented with the space of all possible swing foot positions relative to the stance foot. Steppability is quantified as the maximum velocity perturbation a biped system can sustain such that it can still transition from an SS to another DS contact configuration.

Extending the notion of the BSB, the steppable unbalanced state boundary (SUB) partitions the augmented COM-state space. Whereas the BSB characterizes the system's ability to remain "stable" within a specified contact configuration, the SUB discriminates between a desirable unbalanced state leading to a planned footstep (a steppable state) and an undesirable unbalanced state leading to inevitable falling or an unintended footstep.

Off-line computations of steppability are tractable and can be performed on full-order models with a complete centroidal dynamics formulation. This allows the angular momentum contribution of swing limbs to be considered without the usual treatment through simplified models such as flywheels employed by some capturability-based approaches. While only forward stepping and forward velocity perturbations are considered in this work, the general

case of stepping backwards (or other directions relative to the perturbation velocity) or even the opposite DS to SS transition may be considered with the general framework presented here.

III. Formulation

The construction of the SS BSB, DS BSB, and SUB requires the solution of a series of constrained optimization problems formulated as follows:

A. Constraints

The humanoid robot and human are modeled as systems of rigid bodies subject to the following kinematic, physics-based, and system-specific constraints that are common to the construction of the SS BSB, DS BSB, and SUB [20]:

$$-fl/2 \le M_{\text{stance},z}/F_{\text{stance},y} \le fl/2 \quad \text{for humanoid (SS BSB, SUB)} \quad (1)$$
$$-fl/2 \le M_{\text{swing},z}/F_{\text{swing},y} \le fl/2 \quad \text{(DS BSB)}$$
$$-fl \le M_{\text{stance},z}/F_{\text{stance},y} \le 0 \quad \text{for human (SS BSB, SUB)}$$
$$-fl \le M_{\text{swing},z}/F_{\text{swing},y} \le 0 \quad \text{(DS BSB)}$$
$$\mathbf{q}^{LB} \le \mathbf{q} \le \mathbf{q}^{UB} \quad \text{joint kinematic (angle) limits} \quad (2)$$
$$\dot{\mathbf{q}}^{LB} \le \dot{\mathbf{q}} \le \dot{\mathbf{q}}^{UB} \quad \text{joint kinematic (velocity) limits}$$
$$\boldsymbol{\tau}^{LB}(\dot{\mathbf{q}}) \le \boldsymbol{\tau} \le \boldsymbol{\tau}^{UB}(\dot{\mathbf{q}}) \quad \text{joint actuation (torque) limits}$$
$$F_{\text{stance},y} \ge 0 \quad \text{positive normal contact force} \quad (3)$$
$$F_{\text{swing},y} \ge 0 \quad \text{(DS BSB)}$$
$$\left|F_{\text{stance},x}\right| \le \mu F_{\text{stance},y} \quad \text{friction cone} \quad (4)$$
$$\left|F_{\text{swing},x}\right| \le \mu F_{\text{swing},y} \quad \text{(DS BSB)}$$
$$\mathbf{r}_{\text{stance}} = (0,0) \quad \text{stance foot position} \quad (5)$$
$$r_{\text{swing},y} \ge 0 \quad \text{swing foot position (SS BSB, SUB)} \quad (6)$$
$$\mathbf{r}_{\text{swing}} = (sl_{desired}, 0) \quad \text{(DS BSB)}$$

where fl is the foot length; $M_{\text{stance},z}$, $F_{\text{stance},x}$, $F_{\text{stance},y}$ are the moment, friction force, and normal force applied at the stance foot, respectively; $M_{\text{swing},z}$, $F_{\text{swing},x}$, and $F_{\text{swing},y}$ are the moment, friction force, and normal force applied at the swing foot, respectively; $\mathbf{q}$, $\dot{\mathbf{q}}$, and $\boldsymbol{\tau}$ are the joint variable, velocity, and joint torque vectors, respectively; μ is the coefficient of friction; $r_{\text{stance},x}$ and $r_{\text{stance},y}$ are the X and Y components of the stance foot position vector $\mathbf{r}_{\text{stance}}$; $r_{\text{swing},x}$ and $r_{\text{swing},y}$ are the X and Y components of the swing foot position vector $\mathbf{r}_{\text{swing}}$ position, and $sl_{desired}$ is the desired step length. Note that for DS, the stance foot is the trailing stance foot and the swing foot is the leading stance foot. The superscripts LB and UB indicate lower and upper bounds.

For the construction of the SUB, an additional condition is included to ensure that the system is able to take a step forward. The most direct way to implement this stepping condition is to specify that the swing foot reaches the desired step length at the time instant t_{step} at the end of the solution time interval $[t_0, t_{step}]$ where t_0 is the initial time. However, the solution time interval must be chosen before t_{step} is known. Hence, an interval $[t_0, T]$ is chosen for analysis, where T is a sufficiently large terminal time. The constraints (1)–(6) are only imposed on the interval $[t_0, t_{step}]$ where t_{step} is initialized as T and then updated at every iteration of the optimization procedure. For the construction of the SS and DS BSB, constraints (1)–(6) are imposed for all time. The terminal time T can be chosen to be less than the minimum time needed to place the swing foot on the ground at the desired step length. The swing foot only needs to be positioned at the right distance away from and ahead of the stance foot:

$$\left\{ \exists t_{step} \in [t_0, T] \;\middle|\; \left\|\mathbf{r}_{\text{swing}} - \mathbf{r}_{\text{stance}}\right\| \ge sl_{desired},\; r_{\text{swing},y}(t_{step}) \ge 0, r_{\text{swing},x}(t_{step}) \ge r_{\text{stance},x}(t_{step}) \right\} \quad (7)$$

A final time condition is imposed at T to ensure that (7) is satisfied at least once on the solution time interval.

$$\left\|\mathbf{r}_{\text{swing}}(T) - \mathbf{r}_{\text{stance}}(T)\right\| \ge sl_{desired};\;\; r_{\text{swing},x}(T) \ge r_{\text{stance},x}(T) \quad (8)$$

For the construction of the SUB, (8) is the only final time constraint imposed. For the construction of the DS and SS BSB, final time constraints are imposed such that the system comes to a stop at T while preserving given contacts [20].

B. Algorithm

At each initial COM and swing foot position on a discretized domain, the following optimization problem is formulated to construct the SS BSB, DS BSB, and SUB across the augmented COM-state space:

$$\text{Maximize } \dot{\bar{x}}(t_0) \quad (9)$$

where $\dot{\bar{x}}$ is the X component of the COM velocity $\dot{\bar{\mathbf{r}}}$ at the initial time t_0 and subject to the following constraints:

$$(\bar{x}(t_0), \bar{y}(t_0)) = (x_i, y_j) \quad (10)$$
$$\mathbf{r}_{\text{swing}}(t_0) = (x_{\text{swing},i}, y_{\text{swing},j}) \quad (11)$$

where $\bar{x}$ and $\bar{y}$ are the X and Y components of the COM position vector $\bar{\mathbf{r}}$, respectively; and (x_i, y_j) and $(x_{\text{swing},i}, y_{\text{swing},j})$ are sampled points in augmented COM-state space chosen by some discretization scheme for initial COM and swing foot position, respectively.

Numerical Optimization: The solution of each optimization problem includes the maximized $\dot{\bar{\mathbf{r}}}$ and the corresponding joint kinematics (angle, velocity, and acceleration) over [0, T]. The collocation method is used where the optimization variables are the control vertices of the cubic B-splines used to parameterize joint kinematics [24]. These nonlinear optimization problems are solved as a sequence of sub-problems with the sequential quadratic programming (SQP) method [25]. The terminal time is chosen to be T = 4 s based on results of numerical experiments.

IV. Models

A. General Tree Structure

The DARwIn-OP humanoid robot and a human subject are modeled in the sagittal plane with a tree structure: a multi-body system of rigid links attached to the global reference frame {X, Y, Z} by a three-dimensional floating-base attached at the pelvis (Fig. 1). The floating base

contributes three additional degrees of freedom (DOFs), containing three fictitious joints that represent sagittal-plane rotation and translation.

In each tree structure, only in-plane joint rotations (flexion or extension) during walking were included. Local frames were assigned in accordance with the Denavit-Hartenberg convention such that all joint axes were aligned consistently. The tree structure models of the humanoid and human system have 11 DOFs and 5 branches, and 16 DOFs and 6 branches, respectively. For the humanoid robot, the mass, COM, and inertia tensor of each link were modeled on data obtained from the manufacturer [26] (ROBOTIS Inc.). For the human, the inertial parameters were obtained with an anthropometric model in Visual3D (C-motion) based on the subject's weight and limb lengths.

B. Joint Angle and Actuation Limits

The range of motion of each servomotor in the DARwIn-OP humanoid robot was measured during walking experiments in order to obtain joint angle limits for constraining the humanoid tree structure model. The actuator torque and joint velocity limits of the humanoid were modeled on motor performance parameters provided by the manufacturer [27]. The minimum and maximum joint velocity limits were taken as the negative and positive no-load speed. The minimum and maximum torque limits were taken as the negative and positive stall torque. In addition to stall torque limits, the speed-dependence of the actuator torque in motoring mode was modeled as a linear approximation of the motor torque-speed curve.

The human joint angle limits imposed on the kinematic tree structure were based on normative ranges of motion obtained from the biomechanics literature [28]. The speed and position dependence of the joint torque limits were approximated with regression models of dynamometer data also obtained from the literature [29].

C. Whole-body Angular Momentum

A complete formulation of multi-body system centroidal dynamics is used in order to avoid the deficiencies of previous approaches. The complete inertia tensor is used for each segment of the humanoid and human system instead of the treatment of body segments in previous work as point masses or slender rods with no axial moments of inertia.

Under the rigid body assumption, the angular momentum of each segment is computed properly and efficiently in order to obtain the total rate of change of centroidal angular momentum $\dot{\mathbf{H}}_c$ according to (12), derived from the moment equilibrium of a collection of rigid bodies about their total COM:

$$\mathbf{M}_c = \sum_{k=1}^{N} \boldsymbol{\rho}_k \times m_k \ddot{\boldsymbol{\rho}}_k + \sum_{k=1}^{N} \left(\mathbf{I}_k \dot{\boldsymbol{\omega}}_k + \boldsymbol{\omega}_k \times \mathbf{I}_k \boldsymbol{\omega}_k \right) \tag{12}$$

where k is the link index, m_k is the mass of the k-th link, and N is the total number of links across all branches of the tree structure model. Each term is observed relative to the global reference frame $\{X, Y, Z\}$: $\mathbf{M}_c$ is the resultant moment about the COM of the whole tree structure as observed in $\{X, Y, Z\}$ but written in the COM frame; $\boldsymbol{\omega}_k$ and $\dot{\boldsymbol{\omega}}_k$ are the link angular velocity and acceleration vectors, respectively, written in the link COM frame; $\mathbf{I}_k$ is the link inertia tensor written in the link COM frame; $\boldsymbol{\rho}_k$ and $\ddot{\boldsymbol{\rho}}_k$ are the link COM position and acceleration vector, respectively, written in the COM frame. The origin of each link COM frame is located at its link COM and the origin of the COM frame is located at the COM. The axes of the COM frame and all link COM frames have the same orientation as $\{X, Y, Z\}$. The link COM frame is distinct from the local frame of each link, which is defined according to the Denavit-Hartenberg convention.

Although the recursive Lagrangian multi-body dynamics solver used for optimization is implemented in joint space, the centroidal angular momentum formulation is developed in Cartesian space. The Cartesian vectors $\boldsymbol{\omega}_k$ and $\dot{\boldsymbol{\omega}}_k$ are computed from the homogeneous transformation matrices used in the joint-space dynamics calculations and their derivatives. The following derivation makes use of the skew-symmetric angular velocity matrix $\tilde{\omega}$ and angular acceleration matrix $\dot{\tilde{\omega}}$, which are the Hodge duals of the angular velocity vector $\boldsymbol{\omega} = \begin{bmatrix} \omega_x & \omega_y & \omega_z \end{bmatrix}^T$ and angular acceleration vector $\dot{\boldsymbol{\omega}} = \begin{bmatrix} \dot{\omega}_x & \dot{\omega}_y & \dot{\omega}_z \end{bmatrix}^T$, respectively. The following notation is used [30]:

$$\tilde{\omega} = \begin{bmatrix} 0 & -\omega_z & \omega_y \\ \omega_z & 0 & -\omega_x \\ -\omega_y & \omega_x & 0 \end{bmatrix}; \quad \dot{\tilde{\omega}} = \begin{bmatrix} 0 & -\dot{\omega}_z & \dot{\omega}_y \\ \dot{\omega}_z & 0 & -\dot{\omega}_x \\ -\dot{\omega}_y & \dot{\omega}_x & 0 \end{bmatrix} \tag{13}$$

where the Hodge dual is denoted with a tilde. For convenience, the link index subscript k has been omitted.

Both $\tilde{\omega}$ and $\dot{\tilde{\omega}}$ are directly obtained from R, the rotational transformation matrix that maps from the global reference frame to the k-th local link frame, as follows:

$$\tilde{\omega} = \dot{R}R^T; \quad \dot{\tilde{\omega}} = \ddot{R}R^T - \tilde{\omega}^2 \tag{14}$$

The homogenous transformation matrix A_k maps from global reference frame to the k-th link frame. The first and second derivative of A_k are the joint velocity matrix B_k and the joint acceleration matrix C_k. The 3x3 matrices R_k, $\dot{R}_k$, and $\ddot{R}_k$ used in (14) to compute the angular velocity and acceleration matrices are the upper-left submatrices of A_k, B_k, and C_k. The desired vectors $\boldsymbol{\omega}_k$ and $\dot{\boldsymbol{\omega}}_k$ are then extracted from $\tilde{\omega}$ and $\dot{\tilde{\omega}}$ by selecting and reordering the appropriate entries of the Hodge dual as indicated in (13). The link inertia tensor $\mathbf{I}_k$ can be rewritten as the transformed version of $\mathbf{I}'_k$, the link inertia tensor whose components are computed with respect to the link local frame, directly obtained from manufacturer data or anthropometric formulas. The original centroidal angular momentum equation can then be expressed as follows [30]:

$$\dot{\mathbf{H}}_c = \sum_{k=1}^{n} \boldsymbol{\rho}_k \times m_k \ddot{\boldsymbol{\rho}}_k + \sum_{k=1}^{n} \left(A_k \mathbf{I}'_k A_k{}^T \dot{\boldsymbol{\omega}}_k + \tilde{\omega} A_k \mathbf{I}'_k A_k{}^T \boldsymbol{\omega}_k \right) \quad (15)$$

D. Contact Wrench Distribution

During the transition from the SS to DS contact configuration, only one foot is in full contact with the ground, which restricts the base of support to just the length of the foot. As a result, no scheme for computing the contact wrench distribution across multiple feet is required for computing the SUB because there is no mechanical indeterminacy. However, the total set of steppable unbalanced states are defined as those which are not just steppable but also lie outside of the SS and DS BSB, the latter of which does require a scheme for contact wrench distribution. In the case of the DS contact configuration, both feet remain in contact with the ground and the base of support extends to the convex hull of both leading and trailing stance feet.

In the sagittal plane, there are only three unknowns when the humanoid or human system is in the SS contact configuration, as are the conditions for computing the SS BSB and SUB. These are the two reaction forces and one moment applied at the stance foot, which are as follows [20]:

$$F_{\text{stance},x} = m\ddot{\bar{x}}; \quad F_{\text{stance},y} = m(\ddot{\bar{y}} + g); \quad (16)$$
$$M_{\text{stance},z} = \dot{H}_{c,z} - (r_{\text{stance},x} - \bar{x}) F_{\text{stance},y} + (r_{\text{stance},y} - \bar{y}) F_{\text{stance},x}$$
$$(F_{\text{swing},x}, F_{\text{swing},y}, M_{\text{swing},z}) = (0,0,0)$$

where $\ddot{\bar{x}}$ and $\ddot{\bar{y}}$ are the X and Y components of the COM acceleration vector, respectively.

If there are two feet in contact with the ground, the unknown reactions can only be resolved with approximation or solved for within an optimization problem as follows [20]:

$$F_{\text{stance},x} = (2\beta - 1)\mu_1 F_{\text{stance},y}; \quad F_{\text{stance},y} = \alpha m(\ddot{\bar{y}} + g); \quad (17)$$
$$M_{\text{stance},z} = \left[\gamma fl + COP_{LB}\right] F_{\text{stance},y}$$
$$F_{\text{swing},x} = m\ddot{\bar{x}} - F_{\text{stance},x}; \quad F_{\text{swing},y} = (1-\alpha) m(\ddot{\bar{y}} + g); \quad (18)$$
$$M_{\text{swing},z} = -M_{\text{stance},z} + \bar{x} F_{\text{stance},y} - \bar{y} F_{\text{stance},x}$$
$$-(sl_{desired} - \bar{x}) F_{\text{swing},y} - \bar{y} F_{\text{swing},x} + \dot{H}_{c,z}$$

where $\alpha(t)$, $\beta(t)$, and $\gamma(t)$ are non-dimensionalized optimization variables in the interval [0,1] that determine the relative scaling of the unknown reactions applied on one stance foot versus the other; $\dot{H}_{c,z}$ is the Z component of $\dot{\mathbf{H}}_c$; and COP_{LB} is the lower bound of the trailing stance foot contact region, which is $-fl/2$ and fl for the humanoid and human, respectively.

V. Experimental Methods

Walking experiments were conducted for the DARwIn-OP humanoid robot at five different walking speeds. The default gyro feedback controller *walk_tuner* [21] (ROBOTIS Inc.) was used for gait generation. The SS and DS phases were segmented based on sensor data from force sensing resistors embedded in the feet of the robot. One representative step cycle, defined as one complete SS phase followed by one complete DS phase, was selected for analysis from walking trials conducted at the middle speed. The COM kinematics were computed with forward kinematics from the motor encoder data obtained at each DOF. The measured step length of the representative step cycle was 0.057 m.

Walking experiments were conducted for the human (with informed consent) at the subject's preferred walking speed. The joint kinematics were recorded with motion capture using retroreflective markers and the COM kinematics were obtained in post-processing with Visual3D. A total of seven step cycles were averaged to obtain one representative cycle with an average step length of 0.74 m.

VI. Results And Discussion

A. Effects of Angular Momentum on BSBs

To illustrate that the approach outlined here can account for system-specific characteristics, DS BSBs were obtained for two conditions: unconstrained and constrained arms. In the unconstrained case, the arms were allowed to swing freely within the range set by joint variable limits in the system. In the constrained case, the arms were held rigidly fixed at the sides of the torso.

The BSB results show that arm constraints reduce the balancing capability of the system, as evidenced by the reduction in area of the DS BSB both along the position and velocity axis (Fig. 2). The arm constraints have a positional effect by reducing the system's COM workspace and its ability to maneuver mass, analogous to shifting ballast in order to maintain balance. The arm constraints also have a velocity effect because they restrict the system's capacity to generate angular momentum.

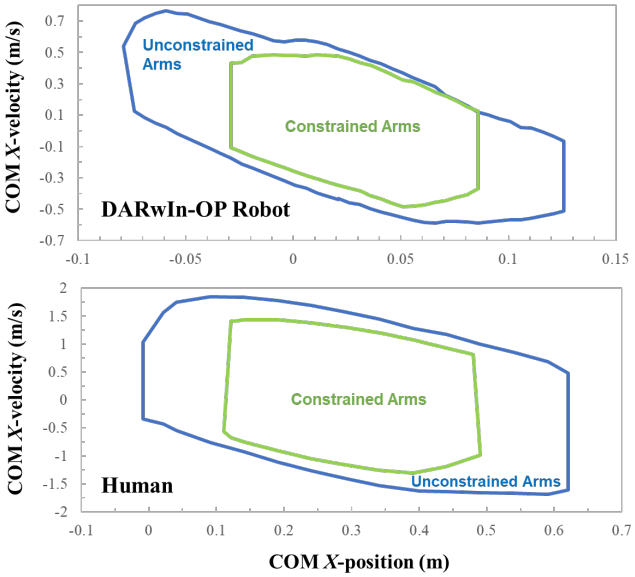

Figure 2. Comparison of unconstrained arms vs. constrained arms DS BSBs for DARwIn-OP humanoid (top) and human (bottom)

B. Humanoid versus Human SUB

In this part, a complete steppability analysis of a representative step cycle is presented for both the humanoid

and human system. Each SUB is presented with the BSB of the initial SS contact configuration starting from a given swing foot location, the BSB of the final DS contact configuration ending at the desired step length, and the experimental walking trajectory in COM-state space. In this work, only the X components of COM-state space were considered. The swing foot, COM X, and COM Y coordinate trajectories of the representative step cycle were sampled to obtain a discretized domain for evaluating each SUB, SS BSB, and DS BSB, allowing for direct comparison between computational and experimental results. The shaded region between the SUB and the SS and DS BSBs for the SS and DS portions of the COM X trajectory represent the set of steppable unbalanced states along the step cycle.

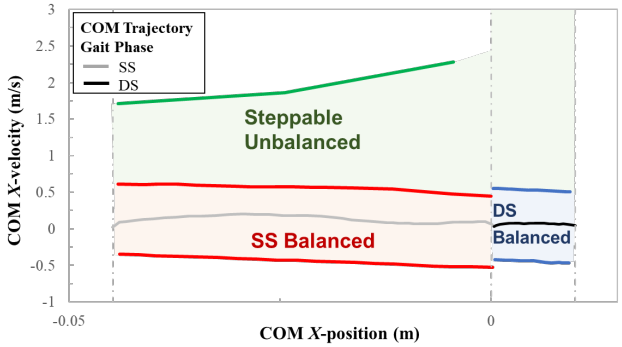

Figure 3. Comparison of the DARwIn-OP humanoid robot SUB, SS BSB, and DS BSB with respect to an experimental COM X trajectory of a representative step cycle. Results are obtained for a step length of 0.057 m. Walking progression is in the direction of increasing COM X-position.

Steppability changes across the progression of a step cycle and increases as the swing foot location approaches the final DS contact configuration (Figs. 3 and 4). When the system enters DS, steppability is effectively infinite because the system has already stepped.

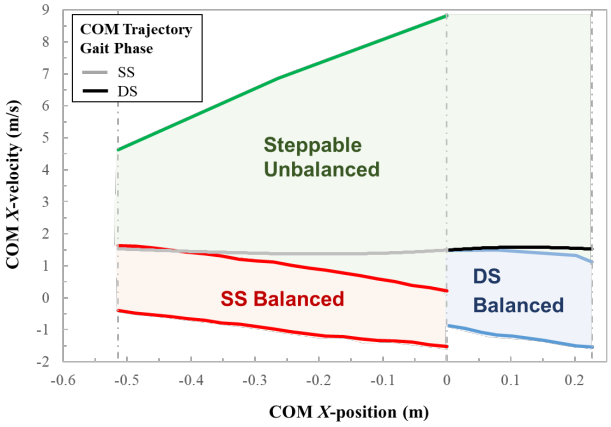

Figure 4. Comparison of the human SUB, SS BSB, and DS BSB with respect to an experimental COM X trajectory of a representative step cycle. Results are obtained for a step length of 0.74 m. Walking progression is in the direction of increasing COM X-position.

Humanoid gait typically employs walking controllers that exhibit conservative walking motions that do not explore the possibility of dynamically balanced locomotion [31]. This is apparent in the comparison with the experimental COM X trajectory, which does not even approach the shaded SUB region when transitioning from SS to DS during gait (Fig. 3).

In the case of human gait, the COM X trajectory lies outside the SS and DS BSB regions and is well within the region of steppable unbalanced states (Fig. 4). During the DS phase, the COM X trajectory is highly unbalanced, indicating that the highly dynamic forward progression is bound to require the detachment of the trailing foot, as expected for normal human walking.

The SUB, when complemented with BSB analysis, provides a refined analysis of the stepping process by considering the start, transition, and end of each step separately. In particular, the SUB is a useful tool for benchmarking system or controller performance that allows experimental or simulated trajectories to be compared with respect to the set of balanced and steppable unbalanced states. Future work includes considering steppability analysis across a range of step lengths and applying the analysis iteratively across multiple steps. In addition, the inclusion of lateral dynamics can extend the SUB to consider omnidirectional stepping on a plane rather than steps along the same forward direction.

ACKNOWLEDGMENT

The authors would like to thank Hyun Seok Shin for his help in computing optimization results and data acquisition and processing.

REFERENCES

[1] M. Vukobratović and B. Borovac, "Zero-Moment point - Thirty five years of its life," *International Journal of Humanoid Robotics,* vol. 1, no. 1, pp. 157-173, 2004.

[2] H. Hirukawa, S. Hattori, K. Harada, S. Kajita, K. Kaneko, F. Kanehiro, K. Fujiwara, and M. Morisawa, "A universal stability criterion of the foot contact of legged robots - adios ZMP," *Proc. IEEE int. Conf. on Robotic and Automation*, May 2006, pp 1976-1983.

[3] F. Firmani and E. J. Park, "Theoretical analysis of the states of balance in bipedal walking," *Journal of Biomechanical Engineering,* vol. 135, no. 4, pp. 041003/1-041003/13, April 2013.

[4] J. Pratt and R. Tedrake, "Chapter: Velocity-based stability margins for fast bipedal walking," in *Fast Motions in Biomechanics and Robotics Lecture Notes in Control and Information Sciences*, Vol. 340, Springer Berlin Heidelberg, pp. 299-324, 2006.

[5] Y. Hurmuzlu and C. Basdogan, "On the measurement of dynamic stability of human locomotion," *Journal of Biomechanical Engineering,* vol. 116, no. 1, pp. 30-36, Jan. 1994.

[6] J. B. Dingwell, J. P. Cusumano, D. Sternad, and P. R. Cavanagh, "Slower speeds in patients with diabetic neuropathy lead to improved local dynamic stability of continuous overground walking," *Journal of Biomechanics,* vol. 33, no. 10, pp. 1269-1277, 2000.

[7] D. G. Hobbelen and M. Wisse, "A disturbance rejection measure for limit cycle walkers: The gait sensitivity norm," *IEEE Transactions on Robotics,* vol. 23, no. 6, 2007, pp. 1213-1224.

[8] P. B. Wieber, "On the stability of walking systems," in *Proceedings of the international workshop on humanoid and human friendly robotics*, 2002.

[9] T. Koolen, T. De Boer, J. Rebula, A. Goswami, and J. Pratt, "Capturability-based analysis and control of legged locomotion, Part 1: Theory and application to three simple gait models," *The International Journal of Robotics Research,* vol. 31, no. 9, pp. 1094-1113, 2012.

[10] P. Zaytsev, S. J. Hasaneini, and A. Ruina, "Two steps is enough: no need to plan far ahead for walking balance," in *IEEE International Conference on Robotics and Automation (ICRA)*, Seattle, 2015.

[11] L. Lanari, S. Hutchinson, and L. Marchionni, "Boundedness issues in planning of locomotion trajectories for biped robots," in *Humanoid Robots (Humanoids), 2014 14th IEEE-RAS International Conference on*, 2014.

[12] T. Koolen, M. Posa, and R. Tedrake, "Balance control using center of mass height variation: limitations imposed by unilateral contact," in *In Humanoid Robots (Humanoids), 2016 IEEE-RAS 16th International Conference on*, 2016.

[13] J. Pratt, J. Carff, S. Drakunov, and A. Goswami, "Capture point: A step toward humanoid push recovery," in *Humanoid Robots, 2006 6th IEEE-RAS International Conference on*, 2006.

[14] J. Englsberger, C. Ott, and A. Albu-Schäffer, "Three-dimensional bipedal walking control based on divergent component of motion," in *IEEE Transactions on Robotics*, vol. 35, no. 2, April 2015.

[15] M. Posa, T. Koolen, and R. Tedrake, "Balancing and Step Recovery Capturability via Sums-of-Squares Optimization," in *Robotics: Science and Systems*, 2017.

[16] L. Zhang and C. Fu, "Predicting foot placement for balance through a simple model with swing leg dynamics," *Journal of Biomechanics,* vol. 77, pp. 155-162, 2018.

[17] S. Caron, A. Escande, L. Lanari, and B. Mallein, "Capturability-Based Pattern Generation for Walking with Variable Height," *IEEE Transactions on Robotics*, 2019, pp. 1-20.

[18] A. Del Prete, S. Tonneau, and N. Mansard, "Zero Step Capturability for Legged Robots in Multicontact," *IEEE Transactions on Robotics,* vol. 34, no. 4, 2018, pp. 1021-1034.

[19] J. P. Aubin, Viability theory, Springer Science & Business Media, 2009.

[20] C. Mummolo, W. Z. Peng, C. Gonzalez, and J. H. Kim, "Contact-dependent balance stability of biped robots," *Journal of Mechanisms and Robotics, ASME Transaction,* vol. 10, no. 2, 2018, pp.021009.

[21] C. Mummolo, L. Mangialardi, and J. H. Kim, "Numerical Estimation of Balanced and Falling States for Constrained Legged Systems," *Journal of Nonlinear Science,* vol. 27, no. 4, p. 1291–1323, 2017.

[22] C. Mummolo, L. Mangialardi, and J. H. Kim, "Identification of balanced states for multi-segmental legged robots using reduced-order model," in *Humanoid Robots (Humanoids), 2015 IEEE-RAS 15th International Conference on*, 2015, pp. 914-919.

[23] C. Mummolo, W. Z. Peng, S. Agarwal, R. Griffin, P. D. Neuhaus, and J. H. Kim, "Stability of Mina v2 for Robot-Assisted Balance and Locomotion," *Frontiers in Neurorobotics,* vol. 12, p. 62, 2018.

[24] J. H. Kim, "Optimization of throwing motion planning for whole-body humanoid mechanism: sidearm and maximum distance," *Mechanism and Machine Theory,* vol. 46, no. 4, pp. 438-453, 2011.

[25] P. E. Gill, W. Murray, and M. A. Saunders, "SNOPT: An SQP algorithm for large-scale constrained optimization," *SIAM journal on optimization,* vol. 12, no. 4, pp. 979-1006, 2002.

[26] "http://darwinop.sourceforge.net/," [Online].

[27] ROBOTIS, "ROBOTIS e-Manual v1.31.01," [Online]. Available: http://support.robotis.com/en/product/actuator/dynamixel/mx_series/mx-28at_ar.htm. [Accessed July 2017].

[28] C. C. Norkin and D. J. White, Measurement of joint motion a guide to goniometry, 4th ed., Philadelphia, PA: F. A. Davis, 2009, pp. 425-430.

[29] D. E. Anderson, M. L. Madigan, and M. A. Nussbaum, "Maximum voluntary joint torque as a function of joint angle and angular velocity: Model development and application to the lower limb," *Journal of Biomechanics,* vol. 40, no. 14, pp. 3105-3113, 2007.

[30] W. Z. Peng, C. Mummolo, and J. H. Kim, "Whole-Body Balancing Criteria for Biped Robots in Sagittal Plane," *ASME IDETC/CIE 43rd Mechanisms and Robotics Conference*, Anaheim, CA, August 2019.

[31] C. Mummolo, F. Cursi, and J. H. Kim, "Balanced and falling states for biped systems: Applications to robotic versus human walking stability," in *Humanoids 2016 - IEEE-RAS International Conference on Humanoid Robots*, Cancun, Mexico, 2016.